

Classification of connection graphs of global attractors
for S^1 -equivariant parabolic equations

Carlos Rocha

Instituto Superior Técnico – Universidade de Lisboa
Avenida Rovisco Pais, 1049–001 Lisboa, PORTUGAL
crocha@tecnico.ulisboa.pt
<http://camgsd.tecnico.ulisboa.pt>

version of April 30, 2024

Abstract

We consider the characterization of global attractors \mathcal{A}_f for semiflows generated by scalar one-dimensional semilinear parabolic equations of the form $u_t = u_{xx} + f(u, u_x)$, defined on the circle $x \in S^1$, for a class of reversible nonlinearities. Given two reversible nonlinearities, f_0 and f_1 , with the same lap signature, we prove the existence of a reversible homotopy $f_\tau, 0 \leq \tau \leq 1$, which preserves all heteroclinic connections. Consequently, we obtain a classification of the connection graphs of global attractors in the class of reversible nonlinearities. We also describe bifurcation diagrams which reduce a global attractor \mathcal{A}_1 to the trivial global attractor $\mathcal{A}_0 = \{0\}$.

1 Introduction

Consider the scalar semilinear parabolic equation

$$(1.1) \quad u_t = u_{xx} + f(u, u_x) \quad , \quad x \in S^1 = \mathbb{R}/2\pi\mathbb{Z} \quad ,$$

where the nonlinearity $f = f(u, u_x)$ satisfies appropriate smoothness and dissipative conditions. Then, (1.1) generates a semiflow in the Sobolev space $X = H^s(S^1), s > \frac{3}{2}$, which possesses a nonempty compact *global attractor* $\mathcal{A} \subset X$. For details see [11] and also [3, 26, 27] for initial references. As general references, see [18, 29] for semiflows, and [16, 4, 17] for global attractors.

Stationary solutions of (1.1) satisfy the equation

$$(1.2) \quad 0 = v_{xx} + f(v, v_x) \quad , \quad x \in S^1 \quad ,$$

and are either *homogeneous equilibria* $v(t, x) = e$, where $f(e, 0) = 0$, or *nonhomogeneous stationary waves*, i.e. 2π -periodic solutions of (1.2). In general, (1.1) also features time periodic solutions. These are *rotating waves* $u(t, x) = v(x - ct)$, rotating around the circle S^1 with constant speed $c \neq 0$. Moreover, the nonconstant wave shapes v correspond to the 2π -periodic solutions of the ODE

$$(1.3) \quad 0 = v_{xx} + f(v, v_x) + cv_x \quad .$$

Our first assumption is

(H): all equilibria and periodic orbits of (1.1) are *hyperbolic*.

Hyperbolicity here concerns the sets of equilibria and nonhomogeneous periodic solutions of the semilinear parabolic PDE (1.1). These are, respectively, the sets \mathcal{E} and \mathcal{P} :

$$(1.4) \quad \begin{aligned} \mathcal{E} &= \{\mathbf{e}_j = (e_j, 0) : 1 \leq j \leq n\}, \\ \mathcal{P} &= \{\mathbf{v}_j = (v_j(x), p_j(x)) : v_j(0) = v_j(2\pi), p_j(0) = p_j(2\pi), x \in [0, 2\pi], 1 \leq j \leq q\}, \end{aligned}$$

where $p = v_x$ and q denotes the number of nonhomogeneous periodic solutions properly x -shifted so that $v_j(0) = \min_{x \in [0, 2\pi]} v_j(x)$. We point out that these solutions may have very large Morse indices $i(\mathbf{e}_j) = \dim W^u(\mathbf{e}_j)$ and $i(\mathbf{v}_j) = \dim W^u(\mathbf{v}_j) - 1$, see [11]. In contrast, the equilibria of the related ODE (1.2) has only alternating saddles and centers, all in one-to-one correspondence with the equilibria of (1.1). For example, the first saddle corresponds to the first stable equilibrium \mathbf{e}_1 and the last saddle corresponds to the last stable equilibrium \mathbf{e}_n .

Notice that a nonhomogeneous stationary solution $v = v(\cdot)$ is not isolated, since all its shifted copies $v(\cdot + \theta), \theta \in \mathbb{R}$, are also 2π -periodic solutions of (1.2). Hence, it is not hyperbolic in stricto sensu. To overcome this inconvenience, hyperbolicity in this case is understood as *normal hyperbolicity*, [12, 31].

If all critical elements in $\mathcal{E} \cup \mathcal{P}$ are strictly hyperbolic, i.e. \mathcal{P} does not contain nonhomogeneous stationary solutions, the global attractor \mathcal{A} is a *Sturm attractor* (see [13]) due to the decay property of the *zero number*, [27]. In addition it has the *Morse-Smale* property, [7, 20]. In this case all the *heteroclinic orbit connections* between equilibria and periodic orbits of \mathcal{A} , which all together compose the global attractor, are determined by a *Sturm permutation*, [13, 31]. See also [14] for the initial results on Sturm permutations. Unfortunately, in the S^1 -equivariant case like the reversible class of nonlinearities $f(u, u_x) = f(u, -u_x)$, we are missing a proper Morse-Smale Theorem. Therefore, our results must be restricted to connection equivalence of global attractors postponing orbit equivalence to further research studies. This observation also applies to the statement of Theorem 3 in [31] which needs a correction, addressing connection equivalence of global attractors instead of orbit equivalence.

The existence of two special homotopies of $f(u, u_x)$, which greatly simplify our task, was established by Fiedler, Rocha and Wolfrum in [12]. The first homotopy freezes all rotating orbits to speed $c = 0$, by introducing corotating coordinates with nonuniform wave speed $c = c(v, v_x)$. This homotopy preserves hyperbolicity of all rotating periodic orbits and their spatial periods, therefore preserves the heteroclinic connectivity between them. In addition, the phase portrait of (1.3) with $c = c(v, v_x)$ is *integrable* in the phase plane region corresponding to the *cyclicity set* \mathcal{C} , i.e. the region of all spatially periodic orbits, see [12]. Therefore, for the nonlinearity $f_0(u, u_x)$ with all rotating waves frozen, we obtain a *period map* $T : \mathcal{D} \subset \mathbb{R} \rightarrow \mathbb{R}_+$ where the domain \mathcal{D} corresponds to (the u -values) of the cyclicity set \mathcal{C} .

The second homotopy $f_\tau(u, u_x), \tau \in [0, 1]$, symmetrizes the phase portrait of (1.2) with respect to the v -axis obtaining a reversible nonlinearity $f(u, v) = f(u, -v)$ which is even in v . This homotopy also preserves the hyperbolicity of all homogeneous equilibria and frozen rotating waves. Moreover, due to the integrability of (1.2), the period map obtained for $f_0(u, u_x)$ is invariant under this second homotopy.

Our objective is the classification of the connection graphs of all Sturm global attractors of flows generated by (1.1). This is achieved using the *lap signature class* introduced in

[31, 12]. The lap signature of a period map $T = T(u_0)$ consists of the set of *period lap numbers* of the 2π -periodic solutions of (1.2) endowed with a total order derived from the nesting of the periodic orbits in the phase space (v, v_x) , and their *regular parenthesis structure* (called regular bracket structure in [23, 31]). We notice that the period lap number $\ell(v)$ of $v \in \mathcal{P}$ is half of the zero number: $z(v) = 2\ell(v)$, see [12].

Let $K = (n - 1)/2 + l$ denote the number of connected regions of the cyclicity set \mathcal{C} . Here n denotes the odd number of equilibria and l the number of annular regions. Notice that each equilibrium of (1.1) corresponds to a center or a saddle point of the phase portrait of (1.2). The centers and saddles alternate for increasing values of u_0 , starting and ending with saddles. Then $(n - 1)/2$ is the number of punctured disks encircling the centers. Moreover, l is the number of annular regions which surround more than one single center. This implies that $0 \leq l \leq (n - 3)/2$. See [12].

Finally, a reversible nonlinearity $f = f(u, u_x)$ is of *simple type* if $l = 0$, i.e. if there are no annular regions. This is a slightly more restrictive definition than the one used in [31]. If $l = 0$ then each 2π -periodic orbit of (1.2) encircles exactly one center in the phase plane (v, v_x) .

Let \mathcal{R} denote the space of reversible nonlinearities. Our main result asserts the following:

Theorem 1. *If $f = f(u, u_x) \in \mathcal{R}$ and $g = g(u, u_x) \in \mathcal{R}$ belong to the same lap signature class (see [31, 12]), then there exists a homotopy in \mathcal{R} between f and g which preserves hyperbolicity (H) of all the homogeneous equilibria and (normally hyperbolic) frozen rotating waves.*

The construction of the homotopy is very delicate and needs some clarification in what concerns the proof in [31], which is restricted to nonlinearities of simple type. In the next Sect. 2 we change some aspects of the proof of Theorem 3 in [31] making it simpler and amenable to a generalization to nonlinearities of non-simple type.

In the final Sect. 3 we discuss these results and conclude with the presentation of bifurcation diagrams and connection graphs of global attractors for dynamical systems generated by (1.1). We also describe bifurcation diagrams which reduce a global attractor \mathcal{A}_1 to the trivial global attractor $\mathcal{A}_0 = \{0\}$.

2 Homotopy between $f_0(u, u_x)$ and $f_1(u)$

We first consider the obstructions to the homotopy construction between a reversible nonlinearity $f_0 = f_0(u, u_x)$ and an $f_1 = f_1(u)$ in the class of Hamiltonian systems.

Let $T = T(u_0) : \mathcal{D} \rightarrow \mathbb{R}_+$ denote the period map of a reversible nonlinearity $f = f(u, u_x)$. By continuity, we extend \mathcal{D} to $u_0 = e$ corresponding to the center $(e, 0)$ which is encircled by periodic orbits. For simplicity, by a translation $u \mapsto u - e$ we let $e = 0$.

A necessary and sufficient condition for $T = T(u_0)$ to be realizable by a Hamiltonian nonlinearity $g = g(u)$ is

$$(C): \quad d(u_0 T(u_0))/du_0 > 0, u_0 \in \mathcal{D}.$$

For references see Theorem 4.2.5 and Proposition 4.2.6 of [32], Theorem 4.2 of [14], and [31].

We first show the existence of reversible nonlinearities $f = f(u, u_x)$ for which this condition is not satisfied. For this purpose, consider the nonlinearity

$$(2.1) \quad f(u, u_x) = \frac{1}{k}u \left(ku^2 + \sqrt{k^2u^4 + 4u_x^2} \right) .$$

Each level curve of the first integral $I(u, v) = \frac{k}{2}u \left(ku^2 + \sqrt{k^2u^4 + 4v^2} \right)$ of (1.2) is an ellipse $v^2 + kI_0u^2 = I_0$ where $I_0 := I(u_0, 0) = ku_0^2$. Therefore, the period map for this nonlinearity is given by

$$(2.2) \quad T(u_0) = 4 \int_0^{u_0} \frac{du}{k\sqrt{u_0^4 - u_0^2u^2}} = \frac{2\pi}{k|u_0|} , \quad u_0 \neq 0 .$$

Hence, since $d(u_0T(u_0))/du_0 = 0$ for $u_0 \neq 0$, condition (C) is not satisfied.

If the period map $T(u_0)$ satisfies condition (C) we are able to find a Hamiltonian nonlinearity $g(u)$ with the same period map, [30]. See also [33, 32] for the preliminary results. In this case, the convex combination

$$(2.3) \quad f_\tau(u, u_x) = (1 - \tau)f(u, u_x) + \tau g(u)$$

realizes the desired homotopy in the Hamiltonian class of nonlinearities.

On the other hand, the failing of condition (C) prevents the homotopy realization in the Hamiltonian class since the period map is not realizable in this class. Therefore, the homotopy has to be constructed directly in \mathcal{R} using the phase portrait of (1.2). We define the homotopy as a continuous transformation of the cyclicity set \mathcal{C} of $f(u, u_x)$, which preserves the hyperbolicity of all homogeneous equilibria and frozen rotating waves, and shrinks the period map along the u -axis until it satisfies condition (C).

Proof of Theorem 1: First, let $f_1(u, u_x)$ denote a reversible nonlinearity such that its time map $T = T(u_0)$ is realizable by a Hamiltonian nonlinearity $g = g(u)$. Also, let G denote the potential function of (1.2), i.e. $G' = g$. Under the hyperbolicity assumption (H) for (1.1) with $f = f_1(u, u_x)$, all the zeros of g are nondegenerate (i.e. $g(u_0) = 0$ implies $g'(u_0) \neq 0$). Moreover, the period map $T = T(u_0)$ satisfies the nondegeneracy condition: $T(u_0) = \frac{2\pi}{k}$ implies $T'(u_0) \neq 0$ for all positive integers $k \in \mathbb{N}$. See [30] for details.

For simplicity, we make here the generic assumption

(M): the potential function G is a *Morse function*.

Hence, in addition to the nondegeneracy of the zeros of g , we also assume that all the critical values of G are distinct ($g(u_0) = g(u_1) = 0$ implies $G(u_0) \neq G(u_1)$). Since we can always add a small perturbation to f_1 , this generic assumption does not affect our result. Initially, we consider that the lap signature class of $f(u, u_x)$ is of simple type. This implies that $l = 0$ and we deal with a cyclicity set composed only of isolated punctured disks around the centers in the phase portrait.

The proof essentially consists on the construction of a homotopy in \mathcal{R} between $f_0(u, u_x)$ and a nonlinearity $f_1(u, u_x)$ satisfying condition (C) of a Hamiltonian nonlinearity $g = g_1(u)$. This homotopy preserves: (a) hyperbolicity of all critical elements of the flow generated by (1.1) with $f = f_0(u, u_x)$; and hence, (b) the lap signature of the period map $T = T_f$.

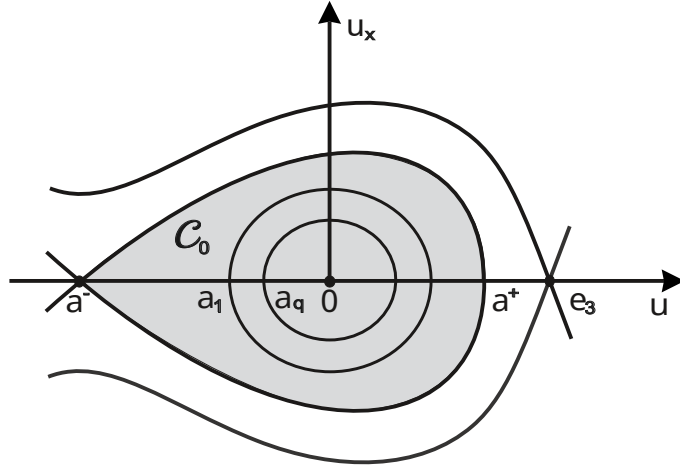


Figure 1: Cyclicity set \mathcal{C}_0 in the case of $n = 3, l = 0$ and with $q = 2$ 2π -periodic orbits.

We consider first the case of a single connected cyclicity set \mathcal{C}_0 surrounding a unique center, *Case (I)*, and then we consider the case of multiple isolated punctured disks, *Case (II)*. Later on we will treat the case of nonlinearities with lap signature class of non-simple type.

Case (I): $n = 3$ and $l = 0$. For the reversible nonlinearity $f = f_0(u, u_x)$ let $e_1 < e_2 = 0 < e_3$ denote the three zeros of $f_0(\cdot, 0)$ corresponding to two saddle points, $\mathbf{e}_1, \mathbf{e}_3$, and a center at the origin $\mathbf{e}_2 = (0, 0)$. The boundary $\partial\mathcal{C}_0$ of the cyclicity set is given by a saddle point and an orbit homoclinic to this saddle. Without loss of generality we assume that the saddle point is \mathbf{e}_1 . Therefore, the cyclicity set \mathcal{C}_0 is positioned to the right of \mathbf{e}_1 , see Fig. 1.

For simplicity we define the interval (a^-, a^+) corresponding to the u -values of the cyclicity set \mathcal{C}_0 . Here $a^- := e_1$ and $a^+, 0 < a^+ < e_3$, corresponds to the maximum u -value of the homoclinic orbit. Then, the period map for $f_0(u, u_x)$ satisfies $T : (a^-, 0) \cup (0, a^+) \rightarrow \mathbb{R}$ and we extend the domain of $T(u_0)$ to $u_0 = 0$ by continuity. By the hyperbolicity assumption (H) and the smoothness of $f_0(u, u_x)$ we obtain,

$$(2.4) \quad T(0) \in \left(\frac{2\pi}{k}, \frac{2\pi}{k-1} \right) \quad \text{for some } k \in \mathbb{N}, \quad \text{and } T'(0) = 0,$$

see for example [32].

Assume the set of periodic solutions \mathcal{P} to be nonempty, i.e. $q \geq 1$. We recall that the frozen rotating waves of $f_0(u, u_x)$ are the 2π -periodic solutions of (1.2), $\mathbf{v}_j \in \mathcal{P}$ for $1 \leq j \leq q$. Let $a_j = \min_{x \in [0, 2\pi]} v_j(x)$ denote the minimal initial values of the u -coordinates of these 2π -periodic solutions. Then, we have $a^- < a_1 < \dots < a_q < 0$ and for each $1 \leq j \leq q$ we have $T(a_j) = \frac{2\pi}{k_j}$ for some $k_j \in \mathbb{N}$.

The proof of case (I) then proceeds by the construction of a homotopy between f_0 and a reversible f_1 which preserves hyperbolicity (H) and for which the period map $T = T_1(a)$ satisfies condition (C). This involves the use of a local diffeomorphism of the plane (u, u_x) which preserves the period map values. Based on [11], Lemma 5.1, this diffeomorphism is described in [31], Sect. 5, and is recalled here for the benefit of the reader.

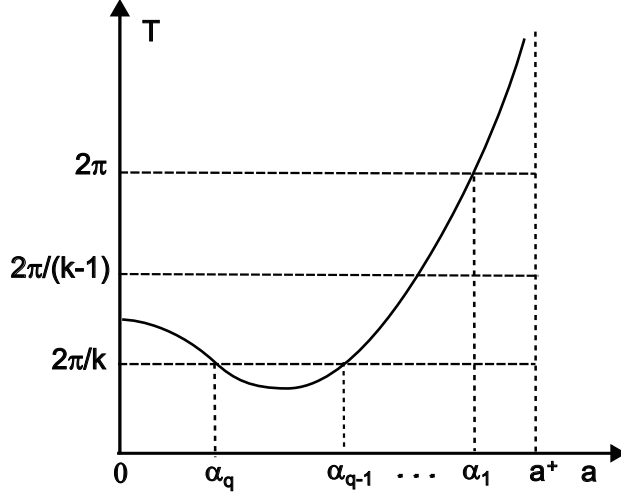


Figure 2: Graph of the period map $T = T(a)$ on the half interval $(0, a^+)$. Here $\alpha_j = \max_{x \in [0, 2\pi]} v_j(x, a_j)$, $j = 1, \dots, q$, denote the maximal values of the 2π -periodic solutions.

Let $(v, p(v)) = (v(\cdot, a), p(v(\cdot, a)))$ denote the periodic orbits of (1.2) on the phase plane (u, u_x) where $v = v(\cdot, a)$ denotes the solution with $v(0, a) = a, v_x(0, a) > 0$. On the cyclicity set \mathcal{C}_0 we define the scaling map

$$(2.5) \quad \Phi(v, p) = \Omega(v, p)(v, p)$$

where $\Omega : \mathcal{C}_0 \rightarrow \mathbb{R}$ is constant along the periodic orbits of (1.2), i.e.

$$(2.6) \quad \Omega(v(\cdot, a), p(v(\cdot, a))) = \Omega(a, 0) .$$

Then, let $\omega : (0, a^+) \rightarrow \mathbb{R}$ denote the scale function $\omega(a) = \Omega(a, 0)$ which is assumed monotone nondecreasing in order to have Φ as a diffeomorphism on the cyclicity set \mathcal{C}_0 . We extend the domain of ω to the interval (a^-, a^+) using the minimal values of the periodic orbits in the cyclicity set and defining $\omega(0) := \omega(0^+) = \omega(0^-)$. Finally, we extend the diffeomorphism Φ to the whole phase space $(u, u_x) \in \mathbb{R}^2$ by defining Φ as the identity in $\mathbb{R}^2 \setminus \mathcal{C}_0$.

To define the scale function $\omega|_{(0, a^+)}$, let $c_1, c_2 \in (\alpha_1, a^+)$ denote two constants satisfying $\alpha_1 < c_1 < c_2 < a^+$, where again α_1 denotes the maximal value of the outermost 2π -periodic solution $v_1(\cdot, a_1)$. Recall that $\lim_{a \rightarrow a^+} T(a) = +\infty$, hence $T(a) > 2\pi$ for $a \in (\alpha_1, a^+)$, see Fig. 2. Moreover, $T'(a) > 0$ in a neighborhood of a^+ and we always choose c_2 in this neighborhood. Then, for a parameter $\delta \in (0, 1)$, we define

$$(2.7) \quad \omega(a) = \begin{cases} \delta & \text{for } a \in (0, c_1) , \\ C^2\text{-smooth monotone increasing} & \text{for } a \in [c_1, c_2] , \\ 1 & \text{for } a \in (c_2, a^+) . \end{cases}$$

Therefore, with this scale function ω , the diffeomorphism Φ shrinks all the 2π -periodic orbits to a neighborhood of the origin as δ decreases, see Fig. 3. Moreover, the period map $T_1(a)$ satisfies

$$(2.8) \quad T_1(a) = T(\omega(a)a) .$$

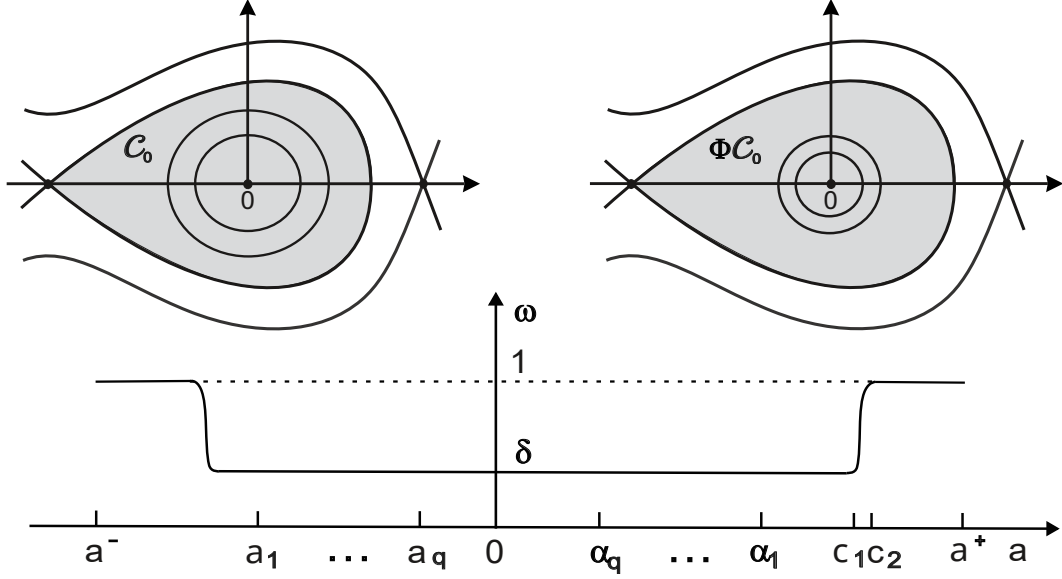


Figure 3: Upper left: Cyclicity set \mathcal{C}_0 for $f = f_0(u, u_x)$. Upper right: Cyclicity set $\Phi\mathcal{C}_0$ for $f = f_1(u, u_x)$. Bottom: Graph of the scale function ω .

Hence, we obtain

$$(2.9) \quad \frac{d}{da} (aT_1(a)) = T(\omega(a)a) + \omega(a)aT'(\omega(a)a) ,$$

which implies that, for δ sufficiently small, $T_1(a)$ satisfies condition (C). Notice that by our choice of c_2 in a neighborhood of a^+ the period map satisfies $T_1'(a) > 0$. We conclude that $f_1(u, u_x)$ is realizable in the Hamiltonian class of nonlinearities completing the proof of case (I).

Case (II): $n \geq 5$ and $l = 0$. Now we deal with a cyclicity set

$$(2.10) \quad \mathcal{C} = \bigcup_{1 \leq k \leq (n+1)/2} \mathcal{C}_k$$

composed of several punctured disks surrounding the $(n+2)/2$ centers of (1.2), see Fig. 4. Since each \mathcal{C}_k is isolated (by condition (M) and the simple type $l = 0$), the proof in this case follows by repeating the previous procedure in each region $\mathcal{C}_k, k = 1, \dots, (n+1)/2$. Therefore, we obtain $(n+1)/2$ disjoint graphs of Hamiltonian realizations, one for each region \mathcal{C}_k . Then, a Hamiltonian $g_1(u)$ which realizes $f_1(u, u_x)$ is obtained by extending the domain to \mathbb{R} joining these g_1 graphs. For this extension, we fill the $(n-3)/2$ closed interval gaps with C^2 -smooth functions without introducing further zeros of g_1 . Similarly, in the two remaining unbounded intervals, our extension choice is such that no further zeros are introduced. Finally, we choose a globally bounded extension $g_1 : \mathbb{R} \rightarrow \mathbb{R}$.

Clearly, $f_0(u, u_x)$ and $g_1(u)$ belong to the same lap signature class. The desired homotopy, then, has the form (see [31]),

$$(2.11) \quad f_\tau(v, p) = \Omega_\tau(v, p) (f_0 \circ \Phi_\tau^{-1}(v, p)) , \quad 0 \leq \tau \leq 1 ,$$

where

$$(2.12) \quad \Phi_\tau(v, p) = \Omega_\tau(v, p) (v, p) , \quad \Omega_\tau(a, 0) = \omega_\tau(a) , \quad \omega_\tau = (1 - \tau) + \tau\omega ,$$

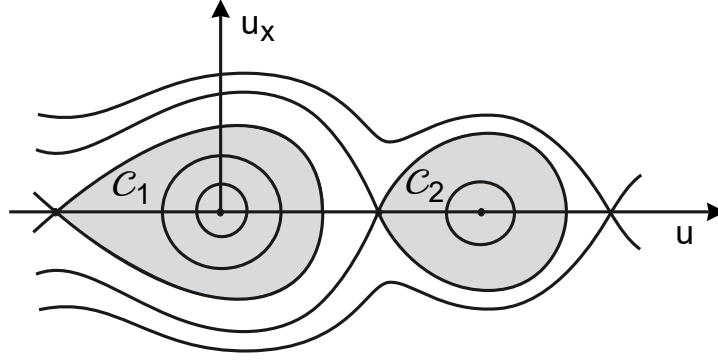


Figure 4: Cyclicity set $\mathcal{C} = \mathcal{C}_1 \cup \mathcal{C}_2$ for $f = f_0(u, u_x)$ with $n = 5$ and $l = 0$.

followed by the homotopy (2.3) between $f_1(u, u_x)$ and $g_1(u)$. Finally, as a result of [31], Theorem 2, (see also [30, 12]), there exists a homotopy between $f(u)$ and $g(u)$ since they belong to the same lap signature class. This completes the proof of case (II).

Remark: Consider again the Hamiltonian realization of $f = f_0(u, u_x)$ by $g_1(u)$ in case (I). The cyclicity set \mathcal{C}_0 is *right oriented* if its boundary $\partial\mathcal{C}_0$ contains the saddle point \mathbf{e}_1 , i.e. $a^- = e_1$. Similarly, \mathcal{C}_0 is *left oriented* if $\partial\mathcal{C}_0$ contains the saddle point \mathbf{e}_3 , i.e. $a^+ = e_3$. Then, if \mathcal{C}_0 is right oriented, the nonlinearity g_1 satisfies $g_1(a^-) = g_1(e_1) = 0$ and is negative for $u \in (a^-, 0)$ and positive for $u \in (0, a^+)$. Therefore, the extension of g_1 to the interval gap (a^+, e_3) is also positive. On the other hand, if \mathcal{C}_0 is left oriented, we have $g_1(e_2) = g_1(a^+) = 0$ and the extension of g_1 to the interval gap (e_1, a^-) is negative. This holds in the multiple case (II) for all the isolated components \mathcal{C}_k of the cyclicity set.

Due to the integrability and the simple type of f_0 the phase portrait of (1.2) for $f = f_0(u, u_x)$ has the following characteristic. There is a saddle point \mathbf{e}_m , $1 \leq m \leq n$ and odd, such that all \mathcal{C}_k to the left of \mathbf{e}_m are right oriented, and all \mathcal{C}_k to the right of \mathbf{e}_m are left oriented. See Fig. 5.

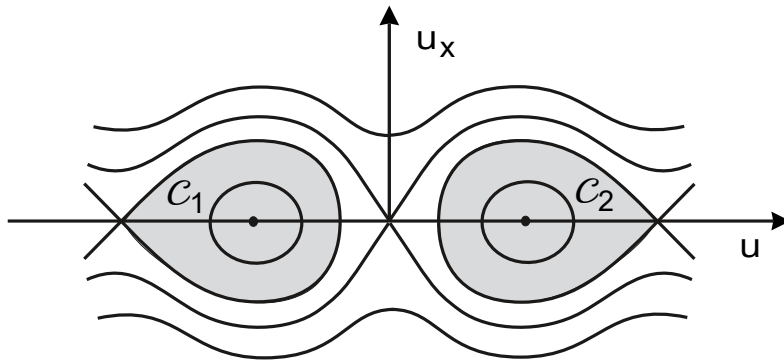


Figure 5: Cyclicity set $\mathcal{C} = \mathcal{C}_1 \cup \mathcal{C}_2$ for $f = f_0(u, u_x)$ with $n = 5$, $l = 0$ and $m = 3$. The previous Fig. 4 illustrates the case $m = n = 5$.

The phase portrait of (1.2) for $f = g_1(u)$ depends essentially on the singular values of the

potential function

$$(2.13) \quad G(a) = \int_{e_2}^a g_1(s) ds$$

at the saddle points, i.e. the local maxima of G , and not on the Morse type of G . Indeed, the Morse type of G is easily modified by changing the values of the extended g_1 in its $(n-1)/2$ closed interval gaps.

Since all \mathcal{C}_k are right oriented at the left of e_m and left oriented at the right, all the extensions of g_1 are positive to the left of e_m and negative to the right. Then, by (2.13), e_m is the saddle point with the maximum value $G(e_m) = \max\{G(e_{2k-1}) : 1 \leq k \leq (n+1)/2\}$ and the sequence of singular values $G(e_{2k-1})$ satisfies the inequalities

$$(2.14) \quad G(e_1) < \dots < G(e_m) \quad , \quad G(e_m) > \dots > G(e_n) \quad .$$

This ensures that the phase portraits of (1.2) for $f = f_0(u, u_x)$ and $f = g_1(u)$ are qualitatively the same.

We now prove the generalization of our main result to the case of nonlinearities with lap signature of non-simple type. We prove this following the same approach used in the previous cases (I) and (II). We first consider the case of \mathcal{C} with a single outermost annular region \mathcal{C}_1 surrounding two cyclicity sets $\mathcal{C}_2 \cup \mathcal{C}_3 = \mathcal{C} \setminus \mathcal{C}_1$, case (III), and then we consider the case of multiple outermost annular regions of \mathcal{C} and punctured disks, case (IV).

In view of the proof of previous cases, we only need to consider nonlinearities $f_0(u, u_x)$ of non-simple type, $l \geq 1$. This implies $n \geq 5$. As before we construct a homotopy in \mathcal{R} between $f_0(u, u_x)$ and a nonlinearity $f_1(u, u_x)$ satisfying condition (C).

Case (III): $n = 5$ and $l = 1$. In this case, the phase portrait of (1.2) for $f = f_0(u, u_x)$ has three cyclicity regions. In addition to two punctured disks $\mathcal{C}_2, \mathcal{C}_3$ surrounding the centers e_2, e_4 , there is an annular region \mathcal{C}_1 surrounding both punctured disks. This implies that the saddle point e_3 has two homoclinic orbits composing the boundary $\partial(\mathcal{C}_2 \cup \mathcal{C}_3)$. The cyclicity regions \mathcal{C}_2 and \mathcal{C}_3 have opposite left/right orientations and the homoclinic orbits form an ∞ shaped curve. See Fig. 6.

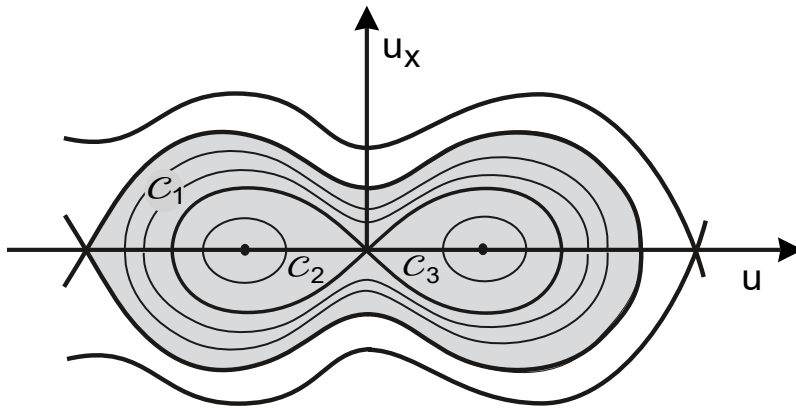


Figure 6: Cyclicity set $\mathcal{C} = \mathcal{C}_1 \cup \mathcal{C}_2 \cup \mathcal{C}_3$ for $f = f_0(u, u_x)$ with $n = 5$, $l = 1$ and $q = 4$. Two of these 2π -periodic orbits are in the annular region \mathcal{C}_1 .

By a translation in u , we assume here that $e_3 = 0$. Therefore, the $n = 5$ equilibria of (1.1) for $f = f_0(u, u_x)$ satisfy $e_1 < e_2 < e_3 = 0 < e_4 < e_5$. We use the same notation that was used in the previous cases. Specifically, we let $(a^-, 0) = (e_1, 0)$ denote the first saddle point, and $(a^+, 0)$ the maximum value of the orbit homoclinic to $(e_1, 0)$. Moreover, we denote by a_1, \dots, a_{q_1} the Neumann initial values of the 2π -periodic orbits $v_j \in \mathcal{P}$ in the annular region \mathcal{C}_1 , i.e. $a_j = \min_{x \in [0, 2\pi]} v_j, 1 \leq j \leq q_1$. Similarly, we denote by $\alpha_1, \dots, \alpha_{q_1}$ the corresponding maximum values $\alpha_j = \max_{x \in [0, 2\pi]} v_j, 1 \leq j \leq q_1$. Notice that in annular regions \mathcal{C}_k the numbers q_k are always even, see [12].

The proof follows the same argument employed in case (I). We use again a shrinking scale function ω which grants the Hamiltonian realization of (2.7) for $f = f_1(u, u_x)$. The essential difference here is the shrinking of all equilibria and 2π -periodic orbits in \mathcal{C} to a neighborhood of the middle saddle point e_3 instead of a neighborhood of the center e_2 .

Then, let again c_1, c_2 , denote the two constants satisfying $\alpha_1 < c_1 < c_2 < a^+$ (c_2 in the appropriate neighborhood of a^+) and, for $\delta \in (0, 1)$, define the scale function ω by (2.7). Once more, using this scale function ω , we define the diffeomorphism $\Phi : \mathcal{C} \rightarrow \mathcal{C}$ which we

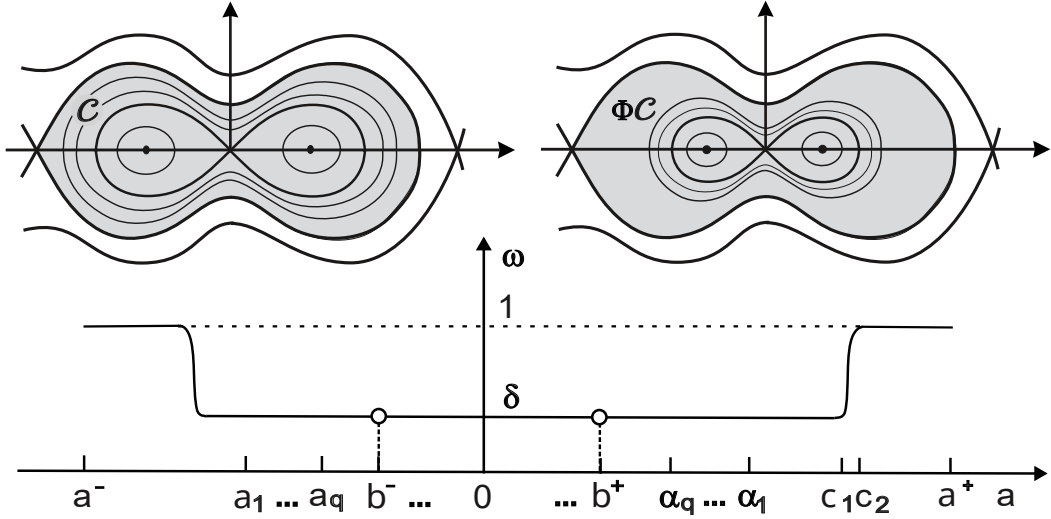


Figure 7: Upper left: Cyclicity set \mathcal{C} for $f = f_0(u, u_x)$. Upper right: Cyclicity set $\Phi\mathcal{C}$ for $f = f_1(u, u_x)$. Bottom: Graph of the scale function ω . Here b^- and b^+ denote respectively the minimum and maximum u -values of the orbits homoclinic to the origin. The white balls correspond to these homoclinic orbits, and $b^\pm \notin \mathcal{D}$ since the homoclinic orbits are not in \mathcal{C} .

extend to $\text{cl } \mathcal{C}$ by continuity, and to the phase plane \mathbb{R}^2 by the identity, $\Phi|(\mathbb{R}^2 \setminus \text{cl } \mathcal{C}) = \text{id}$. As expected, Φ shrinks all equilibria and 2π -periodic orbits in \mathcal{C} to a neighborhood of the origin $(e_3, 0) = (0, 0)$ as δ decreases, preserving hyperbolicity, see Fig. 7. In addition, under Φ the period map T_1 of (1.2) for $f = f_0(u, u_x)$ satisfies (2.8). Then, from (2.9) we again conclude that $T_1(a)$ satisfies condition (C). Hence $f_1(u, u_x)$ is realizable by a Hamiltonian nonlinearity $g_1(u)$ and the desired homotopy from $f_1(u, u_x)$ to $g_1(u)$ has the form (2.11), (2.12), which is followed by the homotopy (2.3). This completes the proof in case (III).

Case (IV): $n \geq 7$ and $l \geq 1$. We proceed sequentially, following the total order imposed by the regular parenthesis structure of the cyclicity regions. For example, the regular

parenthesis structure of the cyclicity region shown in Fig. 6 is

$$(2.15) \quad (()) .$$

The use of the regular parenthesis structure of the cyclicity regions instead of the 2π -periodic orbits is necessary to overcome the case of $l \geq 1$ without 2π -periodic orbits in some annular region \mathcal{C}_k , i.e. $q_k = 0$.

We initially consider the first region $\tilde{\mathcal{C}}$ which may contain the first and outermost 2π -periodic orbit corresponding to the solution with minimal value $a_1 = \min_{x \in [0, 2\pi]} v_1(x, a_1)$. If $\tilde{\mathcal{C}}$ is an isolated punctured disk we apply the scale shrinking procedure described in case (II). So, next we assume that $\tilde{\mathcal{C}}$ is an annular region.

We let \mathcal{C} denote the union of $\tilde{\mathcal{C}}$ with all the cyclicity regions that it encloses. Then, we apply the same argument used in case (III) shrinking all equilibria and 2π -periodic orbits contained in \mathcal{C} to a neighborhood of the unique saddle point in the inner boundary of $\tilde{\mathcal{C}}$. For example, in Fig. 6 the saddle point is \mathbf{e}_3 . Therefore, using the same notation as in case (III), we obtain a diffeomorphism $\Phi : \mathcal{C} \rightarrow \mathcal{C}$ which preserves hyperbolicity and leads to a period map $T_1|_{(a^-, a^+)}$ satisfying condition (C).

Let κ denote the number of annular regions and punctured disks with an outermost homoclinic orbit in their boundaries. Let $\tilde{\mathcal{C}}_k$ denote these either punctured disks or outermost annular regions of the cyclicity set \mathcal{C} . If $\tilde{\mathcal{C}}_k$ is a punctured disk we define $\mathcal{C}_k := \tilde{\mathcal{C}}_k$. If $\tilde{\mathcal{C}}_k$ is an annular region we define $\mathcal{C}_k = \tilde{\mathcal{C}}_k \cup \bar{\mathcal{C}}_k$ where $\bar{\mathcal{C}}_k$ denotes the union of all the cyclicity sets encircled by $\tilde{\mathcal{C}}_k$. In this way we obtain a sequence $\mathcal{C}_1, \dots, \mathcal{C}_\kappa$ where we can apply repeatedly the above procedure. Therefore, we obtain

$$(2.16) \quad \mathcal{C} = \bigcup_{1 \leq k \leq \kappa} \mathcal{C}_k$$

with diffeomorphism $\Phi : \mathcal{C} \rightarrow \mathcal{C}$ which preserves hyperbolicity. Moreover, the period maps $T_1(a)$ restricted to the intervals defined by the maximal homoclinic u -values satisfy condition (C) for δ sufficiently small.

Hence, we again extend Φ to $\text{cl } \mathcal{C}$ by continuity and to the complete phase space $(u, u_x) \in \mathbb{R}^2$ by the identity $\Phi|_{(\mathbb{R}^2 \setminus \text{cl } \mathcal{C})} = \text{id}$. Notice that each \mathcal{C}_k is isolated and, due to this isolation and the integrability of (1.1) for $f = f_1(u, u_x)$, each \mathcal{C}_k accepts the left/right orientation described in the previous Remark after case (II).

We obtain a Hamiltonian realization of (1.2) for $f = f_1(u, u_x)$ by a nonlinearity $g_1(u)$ defined on the isolated intervals determined by the regions \mathcal{C}_k . Then, after the C^2 smooth and globally bounded extension of $g_1(u)$ to \mathbb{R} , filling the unbounded intervals and the interval gaps, we define the potential G by (2.13). Therefore, due to the partial order (2.14) restricted to the saddle points on the boundaries of \mathcal{C}_k , the phase portraits of (1.2) for $f = f_0(u, u_x)$ and $f = g_1(u)$ are qualitatively the same.

Then, preservation of hyperbolicity ensures that $f = f_0(u, u_x)$ and $f = g_1(u)$ belong to the same lap signature class. This completes the proof of case (IV) and concludes the proof of Theorem 1. \square

3 Discussion and concluding remarks

As an application of Theorem 1 we obtain the following result on connection graphs of reversible global attractors

Theorem 2. *Let $f = f(u, u_x)$ and $g = g(u, u_x)$ denote two reversible nonlinearities in the same lap signature class. Then the corresponding global attractors are connection equivalent,*

$$(3.1) \quad \mathcal{A}_f \sim \mathcal{A}_g .$$

Here (3.1) means connection equivalence between global attractors, [9, 10, 31]. This result is not immediate because all the critical elements in \mathcal{P} fail the hyperbolicity condition (H) which would entail the transversality of stable and unstable manifolds and the strong Morse-Smale property. Hence, we replace stable and unstable manifolds by center stable and center unstable manifolds, and prove their automatic transversality following closely the previous transversality results established for the general problem (1.1), see [11, 7]. See also [19, 1] for the original transversality results in the case of separated boundary conditions.

As already mentioned, every 2π -periodic solution in \mathcal{P} is a nonhomogeneous stationary wave frozen in time. So, let \mathcal{F} denote the set of nonhomogeneous stationary waves, and \mathcal{H} the set of heteroclinic orbits. Then, for the restrictive set of reversible nonlinearities $f \in \mathcal{R}$, the global attractor \mathcal{A}_f of (1.1) decomposes as

$$(3.2) \quad \mathcal{A}_f = \mathcal{E} \cup \mathcal{F} \cup \mathcal{H} .$$

By reversibility, each nonhomogeneous stationary solution $v(\cdot) \in \mathcal{F}$ generates a continuum of shifted copies $v(\cdot + \vartheta)$, $\vartheta \in S^1$, all normally hyperbolic. This implies that each $v(\cdot) \in \mathcal{F}$ has a unique center manifold composed by its frozen shifted copies. In view of the gradient flow variational character of (1.1) for $f \in \mathcal{R}$, (see [8]), a non-stationary orbit $u(t, \cdot)$ converges either to equilibria or stationary waves as $t \rightarrow \pm\infty$. Hence, these orbit connections are essentially heteroclinic connections between equilibria, and the proof of transversality is similar to previous proofs not involving periodic orbits. Moreover, the proof of this transversality was already sketched in Propositions 3.1 and 3.2 of [11]. In the following, for each $v(\cdot) \in \mathcal{F}$, we let

$$(3.3) \quad W^{cu}(v(\cdot)) = \bigcup_{\vartheta \in S^1} W^u(v(\cdot + \vartheta)) \quad , \quad W^{cs}(v(\cdot)) = \bigcup_{\vartheta \in S^1} W^s(v(\cdot + \vartheta)) .$$

Finally, we recall that a convenient notion of adjacency between two critical elements in $\mathcal{E} \cup \mathcal{F}$ establishes the existence of heteroclinic orbits, see Theorems 1.3 and 1.4 of [11].

Proof of Theorem 2: In the following, we consider only the case of orbit connections between nonhomogeneous stationary waves since the remaining cases are simpler.

We say that two (different) stationary waves $v_{\pm}(\cdot) \in \mathcal{F}$ are connected by a heteroclinic orbit $u(t, \cdot)$ if this connecting orbit converges to suitably phase shifted stationary waves $w_{\pm} := v_{\pm}(\cdot + \vartheta_{\pm})$ as $t \rightarrow \pm\infty$.

Definition 1: We say that $W^{cu}(v_-)$ and $W^{cs}(v_+)$ are transverse,

$$(3.4) \quad W^{cu}(v_-) \bar{\cap} W^{cs}(v_+) ,$$

if their intersection is empty, or if we have $W^u(w_-) \bar{\cap} W^s(w_+)$.

Let $u_0 = u(0, \cdot)$ denote the initial condition of the connecting orbit. Then, if $S(t) : X \rightarrow X$ denotes the semiflow generated by (1.1), we have that $u(t, x) = S(t)u_0(x)$.

Moreover, if $DS(t)$ is the Fréchet derivative of $S(t)$, then for any $v_0 \in X$ the curve $v(t, \cdot) = (DS(t)u_0(\cdot))v_0(\cdot)$ in X defines the classical solution $v(t, x)$ of the linearized equation

$$(3.5) \quad v_t = v_{xx} + f_p(u, u_x)v_x + f_u(u, u_x)v, \quad x \in S^1, \quad t > 0, \quad v(0, x) = v_0(x).$$

Let $\{\lambda_0 > \lambda_1 > \lambda_2 > \dots\}$ denote the eigenvalues of the linear second order differential operator in (3.5). If $v \in \mathcal{F}$ is a nonhomogeneous stationary wave, then by normal hyperbolicity we define its Morse index $i(v)$ as the number k of strictly positive eigenvalues λ_j . We also have that $\lambda_{k+1} = 0$ corresponds to the eigenfunction $v_{k+1} = v_x$. This shows that

$$(3.6) \quad \dim W^{cu}(v) = i(v) + 1, \quad \text{codim } W^{cs}(v) = i(v).$$

Notice that, if we restrict S^1 to the Neumann interval $[0, \pi]$, then by Sturm-Liouville we conclude that the zero number of the eigenfunction v_j is $z(v_j) = 2j$. Moreover, we recall that the zero number of $v(t, \cdot)$,

$$(3.7) \quad t \mapsto z(v(t, \cdot)),$$

is monotone nonincreasing (see Lemma 2.6 [25]), with strict decreasing at multiple zeros, (see [2]).

For the proof of transversality we follow almost verbatim the proof in [2]. We have the following *zero number characterization of stable and unstable manifolds*, adapted from Lemma 3 and Lemma 4 of [2]:

(i) Let $v \in \mathcal{F}$ have a positive Morse index $i(v) > 0$. Then for each $v_0 \in W^u(v)$ and $k = 1, \dots, i(v)$ there exists a k -dimensional linear subspace $L_k(v_0)$ of the tangent space of $W^u(v)$ at v_0 , $T_{v_0}W^u(v)$, such that for each $w \in L_k(v_0) \setminus \{0\}$ we have $z(w) < 2k$. In particular, if $w \in T_{v_0}W^u(v)$ then $z(w) < 2i(v)$.

(ii) Similarly, let $v_0 \in W^s(v)$ and $w \in T_{v_0}W^s(v) \setminus \{0\}$. Then $z(w) \geq 2i(v)$.

Notice that this characterization immediately precludes the existence of homoclinic connecting orbits. So, we have the following automatic transversality result

Theorem 3. *Let $v_{\pm} \in \mathcal{F}$ denote normally hyperbolic fixed points of the semigroup $S(t)$ defined by (1.1). Then the center unstable manifold of v_- , $W^{cu}(v_-)$, and the center stable manifold of v_+ , $W^{cs}(v_+)$, intersect transversely:*

$$(3.8) \quad W^{cs}(v_+) \bar{\cap} W^{cu}(v_-).$$

This Theorem implies the preservation of heteroclinic orbit connection in the S^1 -equivariant case and entails the connection equivalence (3.1) completing the proof of Theorem 2. \square

Proof of Theorem 3: Recall that if $W^{cu}(v_-) \cap W^{cs}(v_+) = \emptyset$ then, by definition, $W^{cu}(v_-)$ and $W^{cs}(v_+)$ are transverse. So, we assume an intersection point u_0 between the center unstable manifold of v_- and the center stable manifold of v_+ ,

$$(3.9) \quad u_0 \in W^u(w_-) \cap W^s(w_+) \subset W^{cu}(v_-) \cap W^{cs}(v_+).$$

Since the connecting orbit $u(t, \cdot)$ with $u(0, \cdot) = u_0$ lies in $W^u(w_-) \cap W^s(w_+)$, the invariance of these manifolds implies that

$$(3.10) \quad u_t(t, \cdot) \in T_{u_0}W^u(w_-) \cap T_{u_0}W^s(w_+).$$

Moreover, since $u_t(0, \cdot)$ is nonzero, by the zero number characterization of the stable and unstable manifolds we obtain

$$(3.11) \quad 2i(v_+) \leq z(u_t(0, \cdot)) < 2i(v_-) .$$

Let $N = i(v_-)$. Then by the zero number characterization (i) there exists a N -dimensional linear subspace $L_N(u_0) \subset T_{u_0}W^u(w_-)$ such that for any nonzero $w \in L_N(u_0)$ one has

$$(3.12) \quad z(w) < 2N .$$

On the other hand, the nonincreasing property of the zero number implies that for any nonzero $w \in T_{u_0}W^s(w_+)$ we obtain

$$(3.13) \quad z(w) \geq 2N .$$

This shows that

$$(3.14) \quad L_N(u_0) \cap T_{u_0}W^s(w_+) = \{0\} ,$$

and since

$$(3.15) \quad \dim L_N(u_0) = N = \operatorname{codim} T_{u_0}W^s(w_+) ,$$

we obtain

$$(3.16) \quad L_N(u_0) \oplus T_{u_0}W^s(w_+) = X .$$

Hence we have

$$(3.17) \quad T_{u_0}W^u(w_-) + T_{u_0}W^s(w_+) = X$$

which implies $W^u(w_-) \bar{\cap} W^s(w_+)$ and, by our Definition 1, completes the proof of Theorem 3. Notice that forty years ago Dan Henry used the expression “amazing” to refer to this result, and advised the reader to “look at it again”! \square

Theorem 2 is a contribution to the geometric and qualitative theory of dynamical systems generated by parabolic partial differential equations. This result, applied to one-dimensional scalar semilinear PDEs, brings about the classification of these dynamical systems, already initiated in [11, 30, 12, 13]. Similar results are also available in the more complex case of monotone feedback delay differential equations. For results and references see [21, 22, 28].

Clearly, due to Theorem 2, a classification of the global attractors for dynamical systems generated by (1.1) in the reversible class of nonlinearities is provided by the lap signature class. As mentioned in Sect. 1, the lap signature class is given by the set of period lap numbers of the 2π -periodic orbits endowed with the total order derived from the regular parenthesis structure of their nesting in phase space (u, u_x) . This has the form (see [12])

$$(3.18) \quad \left(\{\ell_1^1, \dots, \ell_{k_1}^1\} \left(\{\ell_1^2, \dots, \ell_{k_2}^2\} \left(\dots \right) \dots \left(\{\ell_1^K, \dots, \ell_{k_K}^K\} \right) \right) \right) ,$$

where K again denotes the number of cyclicity regions, k_j denotes the number of 2π -periodic orbits in the j th annular or punctured disk region (this may be empty, in which

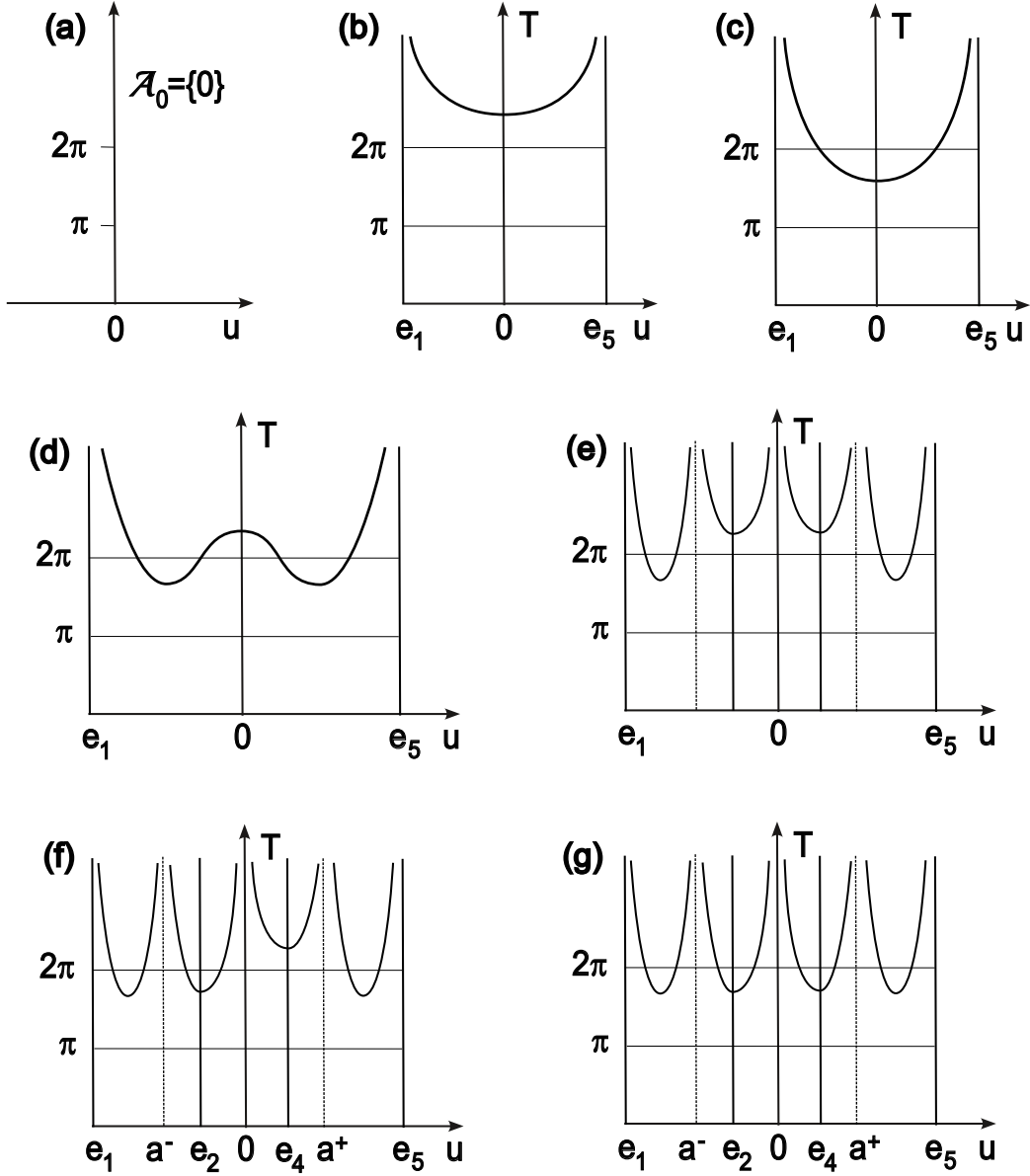


Figure 8: For the global attractor \mathcal{A}_1 of (1.1) with lap signature $(\{1, 1\}(\{1\})(\{1\}))$, we consider the family $f_s \in \mathcal{R}, s \in [0, 1]$ connecting $\mathcal{A}_0 = \{0\}$ to \mathcal{A}_1 . For this example we illustrate the seven period maps which satisfy condition (H). The corresponding s -intervals are: (a) $0 < s < 1/7$; (b) $1/7 < s < 2/7$; (c) $2/7 < s < 3/7$; (d) $3/7 < s < 4/7$; (e) $4/7 < s < 5/7$; (f) $5/7 < s < 6/7$; and, (g) $6/7 < s < 1$. The occurring six bifurcations are discussed in Fig. 9.

case $k_j = 0$), and ℓ_i^j denotes the period lap number of the i th 2π -periodic orbit in the j th cyclicity region. The regular parenthesis structure represents the nesting of the periodic orbits. To illustrate this representation, we exhibit the lap signature class for the example of Fig. 6 (with $n = 5, l = 1, k_1 = 2$ and $k_2 = k_3 = 1$) completing the parenthesis order structure shown in (2.15):

$$(3.19) \quad \left(\{1, 1\} \left(\{1\} \right) \left(\{1\} \right) \right).$$

The present result also shows that in the class of S^1 -equivariant nonlinearities $f = f(u, u_x)$ there is a continuous family of functions $f_s, s \in [0, 1]$, connecting the global Sturm attractors $\mathcal{A}_{f_0} = \{\mathbf{0}\}$ and \mathcal{A}_{f_1} through a finite number of local (degenerate) bifurcations. Here s denotes the bifurcation parameter. Moreover, these bifurcations consist only of pitchfork and Hopf bifurcations. Notice that the bifurcations shown are degenerate because the family $f_s \in \mathcal{R}, s \in [0, 1]$, is entirely constructed in the symmetry class of reversible nonlinearities $f = f(u, u_x)$, which implies its integrability. We also illustrate this bifurcation diagram in the example of Fig. 6. We obtain a family $f_s, s \in [0, 1]$, with six bifurcation points at $s = k/7, 1 \leq k \leq 6$, and seven (degenerate) structurally stable regions $[0, 1] \setminus (\cup_{1 \leq k \leq 6} \{k/7\})$. In Fig. 8 we illustrate the period maps in these seven regions. Since we are restricted to the integrable case $f_s \in \mathcal{R}$, all the bifurcations are degenerate. For general references see [5, 6, 15].

In Fig. 9 we then show the bifurcation diagram from $\mathcal{A}_0 = \{\mathbf{0}\}$ to \mathcal{A}_1 and the connection graph of a nondegenerate global attractor $\tilde{\mathcal{A}}_1$ of (1.1) homotopic to the (degenerate) \mathcal{A}_1 . For this we extend the family f_s to $s > 1$, connecting the reversible (degenerate) \mathcal{A}_1 to a global attractor $\tilde{\mathcal{A}}_1$ which is not reversible, see [12]. In this case $\tilde{\mathcal{A}}_1$ is nondegenerate and we have the usual notions of stability of equilibria and rotation waves, [13]. See [11], Proposition 3.1, and [13], Theorem 10.

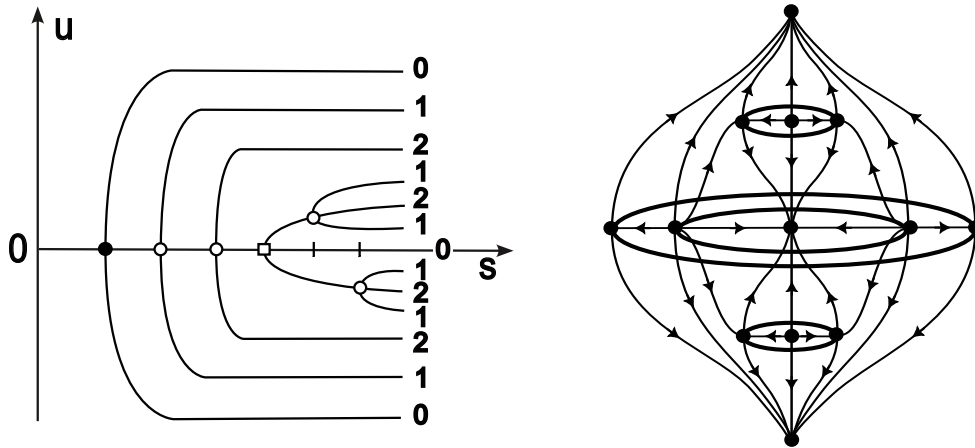


Figure 9: *Left:* The bifurcation diagram for the reversible family $f_s \in \mathcal{R}, s \in [0, 1]$, (see Fig. 8). The bifurcation points are, respectively: a pitchfork of a stable saddle point (black ball); degenerate Hopf bifurcations (white balls); and, a pitchfork of centers (white square). Moreover, the sequence of bifurcations leading to \mathcal{A}_1 are: (i) a supercritical pitchfork bifurcation of two stable saddle points at $s = 1/7$; (ii) a supercritical Hopf bifurcation of an unstable 2π -periodic orbit at $s = 2/7$; (iii) a supercritical Hopf bifurcation of an unstable 2π -periodic orbit at $s = 3/7$; (iv) a supercritical pitchfork bifurcation of two centers at $s = 4/7$; (v) a supercritical Hopf bifurcation of an unstable 2π -periodic orbit at $s = 5/7$ in the upper branch center; and, (v) a supercritical Hopf bifurcation of an unstable 2π -periodic orbit at $s = 6/7$ in the lower branch center. At the right margin of the bifurcation diagram we indicate the Morse indices corresponding to the equilibria and rotating waves of the nondegenerate Neumann section of the global attractor $\tilde{\mathcal{A}}_1$. *Right:* The connection graph of the nondegenerate global attractor $\tilde{\mathcal{A}}_1$.

The global attractor $\tilde{\mathcal{A}}_1$ has three stable equilibria, denoted by $\{\mathbf{e}_1, \mathbf{e}_3 = \mathbf{0}, \mathbf{e}_5\}$, and two

unstable equilibria, $\{\mathbf{e}_2, \mathbf{e}_4\}$, where

$$(3.20) \quad \begin{aligned} \dim W^u(\mathbf{e}_1) &= \dim W^u(\mathbf{e}_3) = \dim W^u(\mathbf{e}_5) = 0, \\ \dim W^u(\mathbf{e}_2) &= \dim W^u(\mathbf{e}_4) = 3. \end{aligned}$$

In addition, there are four rotating waves, denoted $\{\mathbf{v}_1, \mathbf{v}_2, \mathbf{v}_3, \mathbf{v}_4\}$ (by order of appearance). By the normal hyperbolicity of rotating waves, we obtain

$$(3.21) \quad \dim W^u(\mathbf{v}_1) = \dim W^u(\mathbf{v}_3) = \dim W^u(\mathbf{v}_4) = 1, \quad \dim W^u(\mathbf{v}_2) = 2.$$

Therefore, since

$$(3.22) \quad \dim \tilde{\mathcal{A}}_1 = \max\left\{\dim W^u(\mathbf{e}_j), 1 + \dim W^u(\mathbf{v}_k), 1 \leq j \leq 5, 1 \leq k \leq 4\right\} = 3,$$

the global attractor $\tilde{\mathcal{A}}_1$ is three dimensional. The heteroclinic orbit connections follow from the connections on the Neumann section of $\tilde{\mathcal{A}}_1$, [11, 13]. The rotating waves, each one rotating with its own fixed speed c_j , appear on the slow stable/unstable invariant manifolds of the equilibria $\{\mathbf{e}_2, \mathbf{e}_3, \mathbf{e}_4\}$.

We conclude by observing that the connection equivalence of global attractors presented in Theorem 2 extends to the general non-reversible case as orbit equivalence, if we assume that all spatially nonhomogeneous solutions of (1.1) are rotating waves, rotating around the circle S^1 with constant speeds $c_j \neq 0$. In this case, we have $\mathcal{F} = \emptyset$ and all periodic orbits in \mathcal{P} are rotating waves. So, in addition to Theorem 2, we can invoke hyperbolicity (H) and the strong Morse-Smale property.

As a final comment, we believe that Theorem 2 holds for orbit equivalence. To support this statement we observe that a small perturbation $h(u, u_x) = \varepsilon v_x$ breaks reversibility and the orbit equivalence statement holds for the homotopy with $f + h$.

As an application we exhibit the connection graph of the global attractor of (1.1) for the S^1 -equivariant but non-reversible perturbed Chafee-Infante nonlinearity:

$$(3.23) \quad u_t = u_{xx} + \lambda u - u^3 + \varepsilon u_x, \quad x \in S^1, t \geq 0,$$

where $\lambda \neq \lambda_k := k^2, k \in \mathbb{N}$, and $\varepsilon > 0$. The set of equilibria of (3.23), $\mathcal{E} = \{\mathbf{e}_1, \mathbf{e}_2, \mathbf{e}_3\}$, has the equilibria $\mathbf{e}_1 = +\sqrt{\lambda}$ and $\mathbf{e}_3 = -\sqrt{\lambda}$, which are defined and hyperbolic for all $\lambda > 0$. These are saddle points of (1.2). The third equilibrium, $\mathbf{e}_2 = 0$, is also hyperbolic for $\lambda \neq 0, \lambda_k$ and is a center of (1.2).

For $\lambda \in (\lambda_k, \lambda_{k+1})$ the set of periodic orbits $\mathcal{P} = \{v_1, \dots, v_k\}$ has k hyperbolic rotating waves which rotate around S^1 with speed ε and $\mathcal{F} = \emptyset$. Hence, the lap signature of the global attractor \mathcal{A}_λ is

$$(3.24) \quad \left(\{1, \dots, k\}\right),$$

and the connection graph of \mathcal{A}_λ is shown in Fig. 10. As expected, the connection graph of this “spindle attractor” with multiple periodic orbits in his “belt” is a tower, see [24]. By the previous results using normal hyperbolicity this connection graph is preserved for $\varepsilon = 0$, i.e. the reversible case.

ACKNOWLEDGMENTS: The author acknowledges the continuous support of Bernold Fiedler (Freie U. Berlin). I am deeply thankful for his longtime friendship and collaboration. I am also grateful to the continuous support of Isabel Rocha. Without her constant support, this endeavor would not be possible. This work was partially supported by FCT/Portugal through the projects UID/MAT/04459/2019 and UIDB/04459/2020.

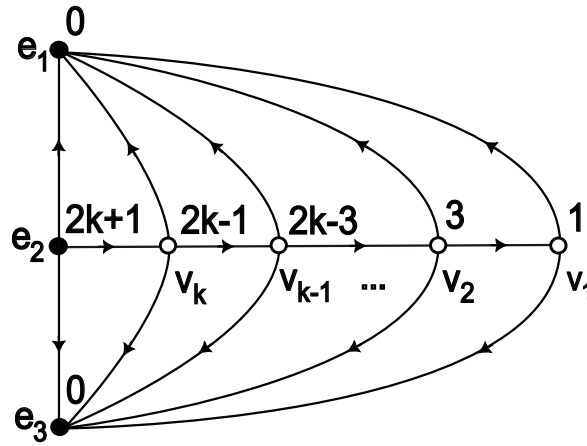


Figure 10: Connection graph of the global attractor \mathcal{A}_λ of (3.23) for $k^2 < \lambda < (k+1)^2$. The numbers close to the edges are the corresponding Morse indices. This shows that $\dim \mathcal{A}_\lambda = 2k+1$.

References

- [1] S. Angenent. The Morse-Smale property for a semi-linear parabolic equation. *J. Differential Equations*, **62** (1986), 427-442.
- [2] S. Angenent. The zero set of a solution of a parabolic equation. *J. reine angew. Math.*, **390** (1988), 79-96.
- [3] S. Angenent and B. Fiedler. The dynamics of rotating waves in scalar reaction diffusion equations. *Trans. Amer. Math. Soc.*, **307** (1988), 545—568.
- [4] A. V. Babin and M. I. Vishik. *Attractors of Evolution Equations*. North Holland, Amsterdam, 1992.
- [5] J. Carr. *Applications of Centre Manifold theory*. Applied Mathematical Sciences 35, Springer-Verlag, New York, Heidelberg, Berlin, 1981.
- [6] S.-N. Chow and J. K. Hale. *Methods of Bifurcation Theory*. Grundlehren der mathematischen Wissenschaften 251, Springer-Verlag, New York, Heidelberg, Berlin, 1982.
- [7] R. Czaja and C. Rocha. Transversality in scalar reaction–diffusion equations on a circle. *J. Differential Equations*, **245** (2008), 692—721.
- [8] B. Fiedler, C. Grotta-Ragazzo and C. Rocha. An explicit Lyapunov function for reflection symmetric parabolic differential equations on the circle. *Russ. Math. Surveys.*, **69** (2014), 419-433.
- [9] B. Fiedler, C. Rocha. Heteroclinic Orbits of Semilinear Parabolic Equations. *J. Differential Equations*, **125** (1996), 239–281.
- [10] B. Fiedler, C. Rocha. Orbit equivalence of global attractors of semilinear parabolic differential equations. *Trans. Amer. Math. Soc.*, **352** (2000), 257–284.

- [11] B. Fiedler, C. Rocha and M. Wolfrum. Heteroclinic orbits between rotating waves of semilinear parabolic equations on the circle. *J. Differential Equations*, **201** (2004), 99–138.
- [12] B. Fiedler, C. Rocha and M. Wolfrum. A permutation characterization of Sturm global attractors of Hamiltonian type. *J. Differential Equations*, **252** (2012), 588–623.
- [13] B. Fiedler, C. Rocha and M. Wolfrum. Sturm global attractors for S^1 -equivariant parabolic equations. *Netw. Heterog. Media*, **7** (2012), 617–659.
- [14] G. Fusco and C. Rocha. A permutation related to the dynamics of a scalar parabolic PDE. *J. Differential Equations*, **91** (1991), 75–94.
- [15] J. Guckenheimer and P. Holmes. *Nonlinear Oscillations, Dynamical Systems, and Bifurcations of Vector Fields*. Applied Mathematical Sciences 42. Springer Science+Business Media, LLC, New York, 1983.
- [16] J. K. Hale. *Asymptotic Behavior of Dissipative Systems*. Math. Surv. **25**. AMS Publications, Providence, 1988.
- [17] J. K. Hale, L. T. Magalhães and W. M. Oliva. *Dynamics in infinite dimensions. Second edition*. Applied Mathematical Sciences, 47. Springer–Verlag, New York, 2002.
- [18] D. Henry. *Geometric Theory of Semilinear Parabolic Equations*. Lect. Notes in Math., Vol. 840. Springer, New York, 1981.
- [19] D. Henry. Some infinite-dimensional Morse-Smale systems defined by parabolic partial differential equations. *J. Differential Equations*, **59** (1985), 165–205.
- [20] R. Joly and G. Raugel, Generic Morse-Smale property for the parabolic equation on a circle. *Ann. I. H. Poincaré – AN*, **27** (2010), 1397–1440.
- [21] T. Krysztin and G. Vas. Large-amplitude periodic solutions for differential equations with delayed monotone positive feedback *J. Dynam. Differential Equations*, **23** (2011), 727–790.
- [22] T. Krysztin and G. Vas. The unstable set of a periodic orbit for delayed positive feedback. *J. Dynam. Differential Equations*, **28** (2016), 805–855.
- [23] S. K. Lando and A. K. Zvonkin. *Graphs on Surfaces and their Applications*. Encyclopaedia of Mathematical Sciences, Low dimensional topology II, Vol. 141. Springer-Verlag Berlin Heidelberg GmbH, 2004.
- [24] R. De Leo and J. A. York. The graph of the logistic map is a tower. *Discrete Contin. Dyn. Syst.*, **41** (2021), 5243–5269.
- [25] H. Matano. Non increase of the lapnumber of a solution for a one dimensional semilinear parabolic equation. *J. Fat. Sci. Univ. Tokyo IA Math.*, **29** (1982), 401–441.

- [26] H. Matano. Asymptotic behavior of solutions of semilinear heat equations on S^1 . In: W. -M. Ni, L. A. Peletier, J. Serrin (Eds.), *Nonlinear Diffusion Equations and their Equilibrium States*, Vol. II, Springer, New York (1988), 139–162.
- [27] H. Matano and K I. Nakamura. The global attractor of semilinear parabolic equations on S^1 . *Discrete Contin. Dyn. Syst.*, **3** (1997), 1–24.
- [28] A. López Nieto. *Enharmonic motion: towards the global dynamics of negative delayed feedback*. PhD Thesis, Freie Universität Berlin, 2023, <https://refubium.fu-berlin.de/handle/fub188/40322>.
- [29] A. Pazy. *Semigroups of Linear Operators and Applications to Partial Differential Equations*. Applied Mathematical Sciences **47**, Springer-Verlag, New York, 1983.
- [30] C. Rocha. Realization of period maps of planar Hamiltonian systems. *J. Dynam. Differential Equations*, **19** (2007), 571–591.
- [31] C. Rocha. Orbit equivalence of global attractors for S^1 -equivariant parabolic equations. *São Paulo J. Math. Sci.*, **6** (2012), 365–374.
- [32] R. Schaaf. *Global solution branches of two point boundary value problems*. Lecture Notes in Mathematics, 1458. Springer-Verlag, New York, 1990.
- [33] M. Urabe. Relations between periods and amplitudes of periodic solutions of $\ddot{x} + g(x) = 0$. *Functial. Ekvac.* **6** (1964), 63–88.